Travel-blocking Optimal Control Policy on Borders of a Chain of Regions Subject to SIRS Discrete Epidemic Model

Sara Bidah[1], **Mostafa Rachik**[1], **Omar Zakary**[1*], **Hamza Boutayeb**[1] and **Ilias Elmouki**[1]

[1]*Department of Mathematics and Computer Sciences, Faculty of Sciences Ben M'Sik, Hassan II University of Casablanca, Avenue Commandant Driss EL HARTI B.P: 7955-Ben M'Sik 20800 Casablanca, Morocco.*

Authors' contributions

This work was carried out in collaboration between all authors. All authors read and approved the final manuscript.

Original Research Article

ABSTRACT

With thousands of people moving from one area to another day by day, in a chain of regions tightly more interconnected than other regions in a given large domain, an epidemic may spread rapidly around it from any point of borders. It might be sometimes urgent to impose travel restrictions to inhibit the spread of infection. As we aim to protect susceptible people of this chain to contact infected travelers coming from its neighbors, we follow the so-called travel-blocking vicinity optimal control approach with the introduction of the notion of patch for representing our targeted group of regions when the epidemic modeling framework is in the form of a Susceptible-Infected-Removed-Susceptible (SIRS) discrete-time system to study the case of the removed class return to susceptibility because of their short-lived immunity. A discrete version of the Pontryagin's maximum principle is employed for the characterization of the travel-blocking optimal control. Finally, with the help of discrete progressive-regressive iterative schemes, we provide cellular simulations of an example of a domain composed with 100 regions and where the targeted chain includes 7 regions.

*Corresponding author: E-mail: zakaryma@gmail.com

1 INTRODUCTION

Susceptible-Infected-Removed-Susceptible (SIRS) compartmental models can model the evolution of different diseases as in [1] which modeled dynamics of the non-typhoidal Salmonella disease, and in the other example [2] which studied the special case of Japanese encephalitis. Generally, these epidemic models are utilized when there is an hypothesis that the removed population could move to the susceptible class after being healed from a disease due to the loss of their immunity. Other studies which were based on SIRS models can be found in [3, 4, 5]. Also, since our modeling framework here, is in the form of a discrete-time SIRS epidemic system, we cite works of Masaki Sekiguchi in [6] and with Emiko Ishiwata in [7]. In fact, as explained in the recently published paper [8] which also deals with SIRS difference equations plus a controlled class compartment, the reason behind such considerations is due to the fact that in epidemics, data are often collected at discrete times.

In order to describe the spatial-temporal dynamics of infection which emerges in different geographical regions and to show the influence of one region on another via infection mobility, a new modeling approach using multi-regions discrete-time epidemic models has been recently presented for this subject in [9, 10], and also in [11, 12, 13, 14] using cellular simulations for the study of this type of models when they are in the form of SIR, S-Exposed-IRS (SEIRS), SEIS and SIS discrete systems respectively. The investigation of the advantages of such epidemic modeling problems has been done for special emerging diseases such as Ebola and Human Immunodeficiency Virus infection and Acquired Immune Deficiency Syndrome (HIV/AIDS) in [15] and [16] respectively.

Here, we deal with the optimal control problem of an epidemic that is described using the model devised in [17] and where the authors tried to exhibit the effectiveness of movements restrictions of the infected individuals coming from the vicinity of a region based on their so-called travel-blocking vicinity optimal control strategy. However, this mentioned reference has not discussed the case when there is an urgent need to control a group of regions or a patch and not only one region. This leads us also to exploit the recent work in [18] and where the notion of patch has been widely explained in the case of SIR model framework. One would still wonder what is the exact difference between the control of a region and the control of a patch here. For this, we start by defining the patch as follows.

Let Ω be our global domain of interest, in form of a grid of M^2 colored cells, uniform in size and connected via movements of their populations. This is just a simplified representation of such connections and which is useful even in the case when these cells are not necessarily joined together. The cells will represent sub-domains of Ω or regions, or more concretely, cities or countries, and we denote them by $(C_{pq})_{p,q=1,..,M}$. Let then the patch be defined by $P = \bigcup\limits_{p,q=1}^{m} C_{pq}$ with $m < M$, subject to a SIRS discrete-time system associated to C_{pq} and with optimal controls functions introduced as effectiveness rates of the travel-blocking operations followed between P and its neighbors. We will need thereafter, the definition of a vicinity set V_{pq} which is composed by all neighboring cells of C_{pq} and which are denoted by $(C_{rs})_{r=p+k,s=q+k'}$ with $(k,k') \in \{-1,0,1\}^2$ except when $k = k' = 0$. Thus, instead of showing the impact of the travel-blocking vicinity optimal approach on reducing contacts between susceptible people of a targeted cell C_{pq} and infected people coming from cells of its vicinity as done in [18], we will be interested here to prove the effectiveness of such policies when they are applied in the borders of the targeted regions chain P with C_{rs} of V_{pq}.

In order to achieve our objective, we apply a discrete version of the Pontryagin's maximum principle for the characterization of the travel-blocking optimal control. Cellular simulations are used to illustrate an example of the application of these modeling and optimal control approaches in a domain composed with 100 regions while the

chain aiming to control includes 7 regions.

2 A DISCRETE-TIME MULTI-REGIONS EPIDEMIC MODEL

As described in introduction, the domain Ω can be defined by $\bigcup\limits_{p,q=1}^{M} C_{pq}$.

We note the susceptibles, infectives and removed people associated to a cell C_{pq} using the states $S_i^{C_{pq}}$, $I_i^{C_{pq}}$, and $R_i^{C_{pq}}$, and we note that the transition between them, is probabilistic, with probabilities being determined by the observed characteristics of specific diseases. In addition to the death, there are population movements among these three epidemiological

compartments, from time unit i to time $i + 1$. Susceptible individuals are assumed to be not yet infected but can be infected only through contacts with infected people from V_{pq}, thus, the infection transmission is assumed to occur between individuals present in a given cell C_{pq}, and is given by

$$\sum_{C_{rs} \in V_{pq}} \beta_{rs} I_i^{C_{rs}} S_i^{C_{pq}}$$

where β_{rs} is the constant proportion of adequate contacts between a susceptible from a cell C_{pq} and an infective coming from its neighbor cell $C_{rs} \in V_{pq}$ with

$V_{pq} = \left\{ C_{rs} \in \Omega / r = p + k, s = q + k', (k, k') \in \{-1, 0, 1\}^2 \right\} \backslash C_{pq}.$

SIRS dynamics associated to domain or cell C_{pq} are described based on the following multi-cells discrete model

For $p, q = 1, \ldots, M$, we have

$$
\begin{aligned}
S_{i+1}^{C_{pq}} &= S_i^{C_{pq}} - \beta_{pq} I_i^{C_{pq}} S_i^{C_{pq}} - \sum_{C_{rs} \in V_{pq}} \beta_{rs} I_i^{C_{rs}} S_i^{C_{pq}} \\
&\quad - dS_i^{C_{pq}} + \theta R_i^{C_{pq}} & (2.1) \\
I_{i+1}^{C_{pq}} &= I_i^{C_{pq}} + \beta_{pq} I_i^{C_{pq}} S_i^{C_{pq}} + \sum_{C_{rs} \in V_{pq}} \beta_{rs} I_i^{C_{rs}} S_i^{C_{pq}} \\
&\quad - (\alpha + \gamma + d) I_i^{C_{pq}} & (2.2) \\
R_{i+1}^{C_{pq}} &= R_i^{C_{pq}} + \gamma I_i^{C_{pq}} - (d + \theta) R_i^{C_{pq}} & (2.3)
\end{aligned}
$$

$i = 0, ..., N - 1$
with $S_0^{C_{pq}} \geq 0, I_0^{C_{pq}} \geq 0$ and $R_0^{C_{pq}} \geq 0$ are the given initial conditions.

Here, $d > 0$ is the natural death rate while $\alpha > 0$ is the death rate due to the infection, $\gamma > 0$ denotes the natural recovery rate from infection and $\theta > 0$ denotes the immunity loss rate. By assuming that is all regions are occupied by homogeneous populations, α, d and γ are considered to be the same for all cells of Ω.

3 A TRAVEL-BLOCKING VICINITY OPTIMAL CONTROL APPROACH

Let $I = \{1, 2, ..., M\}$, $I_H \subset I$ a subset of I, and consider $P = \{C_{pq}/p, q \in I_H\}$ denoting a patch

of controlled cells, with its complementary in Ω, defined as $\bar{P} = \{C_{ij}/i, j \in I \backslash I_H\}$.

The main goal of the travel-blocking vicinity optimal control approach is to restrict movements of infected people coming from the set V_{pq} and aiming to reach the patch P without including cells C_{rs} which belong to $V_{pq} \bigcap P$. For this, we introduce control variables $u^{pqC_{rs}}$ which limits contacts between susceptible of the patch P and infected individuals from cells C_{rs} which belong to $V_{pq} \bigcap \bar{P}$.

In this section, we introduce controls variables in the above mentioned model to restrict contacts between susceptible people of the controlled cells $C_{pq} \in P$ and infected ones which belong to $C_{rs} \in \bar{P} \cap V_{pq}$. Then, for a given cell $C_{pq} \in P$, the discrete-time system (2.1)-(2.2)-(2.3) becomes

$$
S_{i+1}^{C_{pq}} = S_i^{C_{pq}} - \beta_{pq} I_i^{C_{pq}} S_i^{C_{pq}} - \sum_{C_{rs} \in P \cap V_{pq}} \beta_{rs} I_i^{C_{rs}} S_i^{C_{pq}}
$$

$$
- \sum_{C_{rs} \in \bar{P} \cap V_{pq}} u_i^{pq C_{rs}} \beta_{rs} I_i^{C_{rs}} S_i^{C_{pq}} - dS_i^{C_{pq}} + \theta R_i^{C_{pq}} \tag{3.1}
$$

$$
I_{i+1}^{C_{pq}} = I_i^{C_{pq}} + \beta_{pq} I_i^{C_{pq}} S_i^{C_{pq}} + \sum_{C_{rs} \in P \cap V_{pq}} \beta_{rs} I_i^{C_{rs}} S_i^{C_{pq}}
$$

$$
+ \sum_{C_{rs} \in \bar{P} \cap V_{pq}} u_i^{pq C_{rs}} \beta_{rs} I_i^{C_{rs}} S_i^{C_{pq}} - (d + \alpha + \gamma) I_i^{C_{pq}} \tag{3.2}
$$

$$
R_{i+1}^{C_{pq}} = R_i^{C_{pq}} + \gamma I_i^{C_{pq}} - (d + \theta) R_i^{C_{pq}} \tag{3.3}
$$

$i = 0, ..., N - 1$

Since our goal concerns the minimization of the number of the infected people and the cost of the vicinity optimal control approach, we consider an optimization criterion associated to the patch P, and we define it by the following objective function

$$
J_P(u) = \sum_{C_{pq} \in P} \left[A_1 I_N^{C_{pq}} + \sum_{i=0}^{N-1} \left(A_1 I_i^{C_{pq}} + \sum_{C_{rs} \in \bar{P} \cap V_{pq}} \frac{A_{rs}}{2} (u_i^{pq C_{rs}})^2 \right) \right] \tag{3.4}
$$

where $A_1 > 0$ and $A_{rs} > 0$ are the constant severity weights associated to the number of infected individuals and controls respectively.

We note that here, $u = \left(u_i^{pq C_{rs}} \right)_{C_{rs} \in \bar{P} \cap V_{pq}, i=1,...,N-1, p,q \in I_H}$

which belongs to the control set U_P defined as

$$
U_P = \left\{ u / u^{min} \le u_i^{pq C_{rs}} \le u^{max}, \, i = 1, ..., N - 1, \, C_{rs} \in \bar{P} \cap V_{pq} \right\}
$$

Then, we seek optimal control u such that

$$
J_P(u^*) = min\{ J_P(u) / u \in U_P \}
$$

The sufficient conditions for the existence of optimal controls in the case of discrete-time epidemic models have been announced in [8].

As regards to the necessary conditions and the characterization of our discrete optimal control, we use a discrete version of the Pontryagin's maximum principle [19].

For this, we define an Hamiltonian $\mathcal{H}$ associated to a patch P by

$$
\mathcal{H} = \sum_{C_{pq} \in P} \left[A_1 I_i^{C_{pq}} + \sum_{C_{rs} \in \bar{P} \cap V_{pq}} \frac{A_{rs}}{2} (u_i^{pq C_{rs}})^2 \right.
$$

$$
+ \zeta_{1,i+1}^{C_{pq}} \left(S_i^{C_{pq}} - \beta_{pq} I_i^{C_{pq}} S_i^{C_{pq}} - \sum_{C_{rs} \in P \cap V_{pq}} \beta_{rs} I_i^{C_{rs}} S_i^{C_{pq}} \right.
$$

$$
\begin{aligned}
&- \sum_{C_{rs} \in \bar{P} \cap V_{pq}} u_i^{pqC_{rs}} \beta_{rs} I_i^{C_{rs}} S_i^{C_{pq}} - dS_i^{C_{pq}} + \theta R_i^{C_{pq}} \Bigg) \\
&+ \quad \zeta_{2,i+1}^{C_{pq}} \left(I_i^{C_{pq}} + \beta_{pq} I_i^{C_{pq}} S_i^{C_{pq}} + \sum_{C_{rs} \in P \cap V_{pq}} \beta_{rs} I_i^{C_{rs}} S_i^{C_{pq}} \right. \\
&+ \sum_{C_{rs} \in \bar{P} \cap V_{pq}} u_i^{pqC_{rs}} \beta_{rs} I_i^{C_{rs}} S_i^{C_{pq}} - (d + \alpha + \gamma) I_i^{C_{pq}} \Bigg) \\
&+ \quad \zeta_{3,i+1}^{C_{pq}} \left(R_i^{C_{pq}} + \gamma I_i^{C_{pq}} - (d+\theta) R_i^{C_{pq}} \right) \Big]
\end{aligned}
$$

$i = 0, ..., N - 1$

with $\zeta_{k,i}^{C_{pq}}$, $k = 1, 2, 3$, the adjoint variables associated to $S_i^{C_{pq}}$, $I_i^{C_{pq}}$ and $R_i^{C_{pq}}$ respectively, and defined based on formulations of the following theorem.

Theorem 3.1. *(Necessary Conditions & Characterization) Given optimal controls $u^{pqC_{rs}*}$ and solutions $S^{C_{pq}*}, I^{C_{pq}*}$ and $R^{C_{pq}*}$, there exists $\zeta_{k,i}^{C_{pq}}$, $i = 0...N$, $k = 1, 2, 3$, the adjoint variables satisfying the following equations*

$$
\begin{aligned}
\triangle \zeta_{1,i}^{C_{pq}} &= -[(1 - d) \zeta_{1,i+1}^{C_{pq}} + \left(\beta_{pq} I_i^{C_{pq}} + \sum_{C_{rs} \in P \cap V_{pq}} \beta_{rs} I_i^{C_{rs}} + \sum_{C_{rs} \in \bar{P} \cap V_{pq}} u_i^{pqC_{rs}} \beta_{rs} I_i^{C_{rs}} \right) \\
&\quad \times \left(\zeta_{2,i+1}^{C_{pq}} - \zeta_{1,i+1}^{C_{pq}} \right)] \quad (3.5)
\end{aligned}
$$

$$
\triangle \zeta_{2,i}^{C_{pq}} = - \left[A_1 + \beta_{pq} S_i^{C_{pq}} \left(\zeta_{2,i+1}^{C_{pq}} - \zeta_{1,i+1}^{C_{pq}} \right) + (1 - d - \alpha - \gamma) \zeta_{2,i+1}^{C_{pq}} \right] \quad (3.6)
$$

$$
\triangle \zeta_{3,i}^{C_{pq}} = - \left[(1 - d) \zeta_{3,i+1}^{C_{pq}} + \theta \left(\zeta_{1,i+1}^{C_{pq}} - \zeta_{3,i+1}^{C_{pq}} \right) \right] \quad (3.7)
$$

with $\zeta_{1,N}^{C_{pq}} = 0, \zeta_{2,N}^{C_{pq}} = A_1, \zeta_{3,N}^{C_{pq}} = 0$ *are the transversality conditions.*

In addition

$$
\begin{aligned}
u_i^{pqC_{rs}*} &= min \left(max \left(u^{min}, \frac{(\zeta_{1,i+1}^{C_{pq}} - \zeta_{2,i+1}^{C_{pq}}) \beta_{rs} I_i^{C_{rs}*} S_i^{C_{pq}*}}{A_{rs}} \right), u^{max} \right), \\
&\quad i = 0, ..., N - 1, C_{rs} \in V_{pq} \quad (3.8)
\end{aligned}
$$

Proof. Using a discrete version of the Pontryagin's Maximum Principle in [9],[10],[19], and setting $S^{C_{pq}} = S^{C_{pq}*}$, $I^{C_{pq}} = I^{C_{pq}*}$, $R^{C_{pq}} = R^{C_{pq}*}$ and $u^{pqC_{rs}} = u^{pqC_{rs}*}$ we obtain the following adjoint equations

$$
\begin{aligned}
\triangle \zeta_{1,i}^{C_{pq}} \quad &- \quad \frac{\partial \mathcal{H}}{\partial S_i^{C_{pq}}} \\
&= -[(1 - d) \zeta_{1,i+1}^{C_{pq}} + \left(\beta_{pq} I_i^{C_{pq}} + \sum_{C_{rs} \in P \cap V_{pq}} \beta_{rs} I_i^{C_{rs}} + \sum_{C_{rs} \in \bar{P} \cap V_{pq}} u_i^{pqC_{rs}} \beta_{rs} I_i^{C_{rs}} \right) \\
&\quad \times \left(\zeta_{2,i+1}^{C_{pq}} - \zeta_{1,i+1}^{C_{pq}} \right)]
\end{aligned}
$$

$$
\begin{aligned}
\triangle \zeta_{2,i}^{C_{pq}} &= -\frac{\partial \mathcal{H}}{\partial I_i^{C_{pq}}} \\
&= -\left[A_1 + \beta_{pq} S_i^{C_{pq}} \left(\zeta_{2,i+1}^{C_{pq}} - \zeta_{1,i+1}^{C_{pq}} \right) + (1 - d - \alpha - \gamma) \zeta_{2,i+1}^{C_{pq}} \right] \\
\triangle \zeta_{3,i}^{C_{pq}} &= -\frac{\partial \mathcal{H}}{\partial R_i^{C_{pq}}} \\
&= -\left[(1 - d) \zeta_{3,i+1}^{C_{pq}} + \theta \left(\zeta_{1,i+1}^{C_{pq}} - \zeta_{3,i+1}^{C_{pq}} \right) \right]
\end{aligned}
$$

with $\triangle \zeta_{k,i} = \zeta_{k,i+1} - \zeta_{k,i}, \; k = 1,2,3$; the difference operator, and $\zeta_{1,N}^{C_{pq}} = 0, \zeta_{2,N}^{C_{pq}} = A_1, \zeta_{3,N}^{C_{pq}} = 0$; the transversality conditions.

In order to obtain the optimality condition, we calculate the derivative of H with respect to $u_i^{pqC_{rs}}$, and we set it equal to zero

$$
\frac{\partial \mathcal{H}}{\partial u_i^{pqC_{rs}}} = A_{rs} u_i^{pqC_{rs}} - \zeta_{1,i+1}^{C_{pq}} \beta_{rs} I_i^{C_{rs}} S_i^{C_{pq}} + \zeta_{2,i+1}^{C_{pq}} \beta_{rs} I_i^{C_{rs}} S_i^{C_{pq}} = 0
$$

Then, we obtain

$$
u_i^{pqC_{rs}} = \frac{(\zeta_{1,i+1}^{C_{pq}} - \zeta_{2,i+1}^{C_{pq}}) \beta_{rs} I_i^{C_{rs}} S_i^{C_{pq}}}{A_{rs}}
$$

By the bounds in U_P, we finally obtain the characterization of the optimal controls $u_i^{pqC_{rs}*}$ as

$$
\begin{aligned}
u_i^{pqC_{rs}*} &= min \left(max \left(u^{min}, \frac{(\zeta_{1,i+1}^{C_{pq}} - \zeta_{2,i+1}^{C_{pq}}) \beta_{rs} I_i^{C_{rs}*} S_i^{C_{pq}*}}{A_{rs}} \right), u^{max} \right), \\
&\quad i = 0, ..., N - 1, C_{rs} \in V_{pq}
\end{aligned}
$$

$\square$

4 RESULTS

In order to avoid repetitions, we call readers to [11, 12, 13, 14, 17, 18], to understand our programming code used in the simulations below. However, here are some important information to make our comments clearer.

- $M = 10$; $\Omega = 10 \times 10$ grid.
- C_{1010}, the source infection cell, is located at the lower-right corner of Ω.
- $S_0^{C_{pq}} = 50$ except $S_0^{C_{1010}} = 40$.
- $I_0^{C_{pq}} = 0$ except $I_0^{C_{1010}} = 10$.
- $C_{610}, C_{69}, C_{68}, C_{67}, C_{77}, C_{87}$ and C_{97} are cells forming the chain of regions aiming to control.
For other details, see Table 1.

In the absence of control, Fig. 1 depicts dynamics of the number of susceptible people in the 100 regions, starting from an initial condition $S_0^{C_{pq}} = 50$ except in cell C_{1010} located at

the lower right corner of Ω where we suppose $S_0^{C_{1010}} = 40$. After 150 times, we can see that the epidemic has emerged in neighboring regions of C_{1010} and the value of $S^{C_{pq}}$ in this cell has even decreased to a value close/or equal to 22 while it has taken values between 20 and 25 in V_{1010}. As we move away from V_{1010}, these values change from 30 around it, while taking values from 45 to 50 as we go far away towards the opposite corner. In the same figure, at $i = 300$, we can observe that in most cells in and around the infection source corner and the center, $S^{C_{pq}}$ decreases and changes values from 0 to 10, while taking values comprised between 20 to 30 in most cells of further vicinities of the center and values between 35 and 45 in other three corners and their closest vicinities. This means that infection has succeeded to enter to most cells of the considered domain, and the number of infectives has even increased to larger values in further time as we can see at next times.

Table 1. Parameters values of α, β, γ and d with the initial conditions $S_0^{C_{pq}}, I_0^{C_{pq}}$ and $R_0^{C_{pq}}$ associated to any cell C_{pq} of Ω.

$S_0^{C_{pq}}$	$I_0^{C_{pq}}$	$R_0^{C_{pq}}$	α	β	γ	d	θ
50	0	0	0.002	0.0001	0.003	0.0001	0.0002

In Fig. 2, we can observe the evolution of $I^{C_{pq}}$ over 900 times as infection starts from C_{1010} at initial time with 10 infected individuals while other regions are all supposed safe with no sign of infection. At time $i = 150$, the infection starts to increase and takes the value 18 in C_{1010} and values from 20 to 25 in its vicinity while there is yet no sign of infection as we arrive to the center. At $i = 300$, it is almost different and the values comprised between 30 and 35 gain the number of infected people in most cells in the vicinities of the center while it takes the value 25 in C_{1010} and 28 in its vicinity. As we move towards the opposite corner and go far away from the center, the value of $I^{C_{pq}}$ changes from 10 to 20. On the other hand, we should note that at this particular time,

we understand more that as more the infection arrives to cells with larger number of neighbors in their vicinities, as more the infection proves its potential to affect an important number of people compared to the starting value. After 450 days, all cells are now infected taking the value 20 in most cells that are near the center in direction of the source of infection while changing from 25 to 30 in further cells in opposite borders and vicinities of their cells.

In Fig. 3, we can observe that at instant $i = 150$, the value of $R^{C_{pq}}$ has not increased compared to its value at initial time except in the corner and its vicinity with tiny differences as this value does not exceed even three removed individuals.
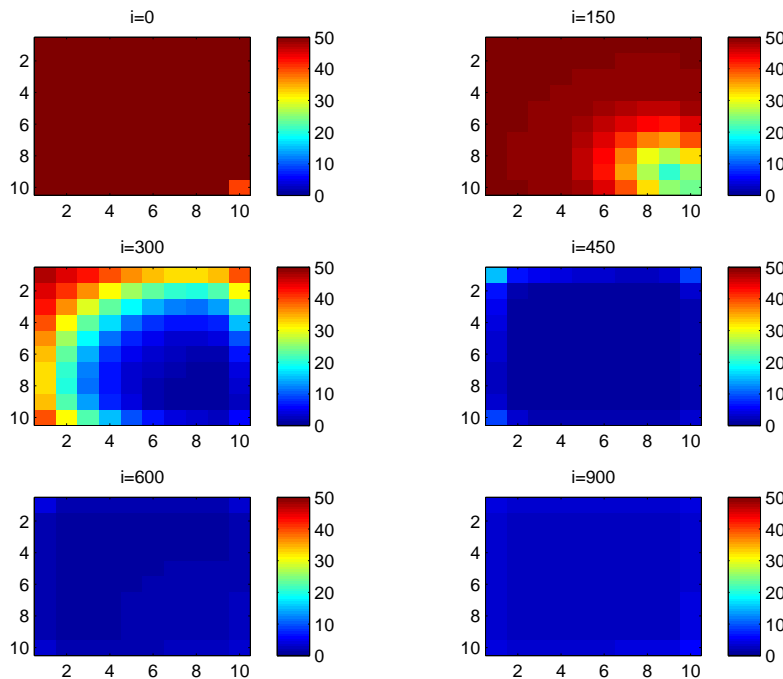
Fig. 1. $S^{C_{pq}}$ **behavior in the absence of controls**

At instant $i = 300$, the number $R^{C_{pq}}$ is not zero in almost cells and is still under the number of 10 people, except for distant cells that are near the other corners where it remains zero. At instant $i = 450$, the value of 10 people chooses the cells in opposite borders while $R^{C_{pq}}$ takes values between 13 and 15 as we move from the center towards C_{1010}. Finally, at further instants, and due to natural recovery of infected people, $R^{C_{pq}}$ increases to 18 individuals in most cells at $i = 600$ while this number decreases at $i = 900$ to 12 people since some people lose their immune responses and move to the susceptible class.

In the presence of controls, we do not see any difference in simulations between Fig. 4 and Fig. 1 at initial time. However, the difference starts to appear after only 150 times, as the number $S^{C_{pq}}$ has not changed in the controlled patch. This number has not decreased as it has done previously in cells that are located at the seventh and under-seventh lines, namely in cells at the left-side border of the patch. An interesting result at this particular time, is that no change

occurred in cells over the patch or at the top border line, or more precisely, the ones located at the fifth line of Ω including the center cell. This means that the travel-blocking vicinity optimal control approach applied to that patch, may also protect its neighbors. The same conclusion can be deduced from this figure at $i = 300$ since even the cells that are either located under or over the controlled patch, have not observed a decrease of $S^{C_{pq}}$ as it has been seen in case without controls.

This leads to a decrease in distant cells at $i = 450$ and that is not important compared to results in Fig. 1. as we understand that since the neighboring cells of the patch are protected, then their vicinities would not observe a significant decrease of $S^{C_{pq}}$. Simulations at further instants, namely at $i = 600$ and $i = 900$, are similar to the ones in Fig. 1. However, the cells in the controlled patch have not lost most of their susceptible people since $S^{C_{pq}}$ has decreased by only 5 individuals.
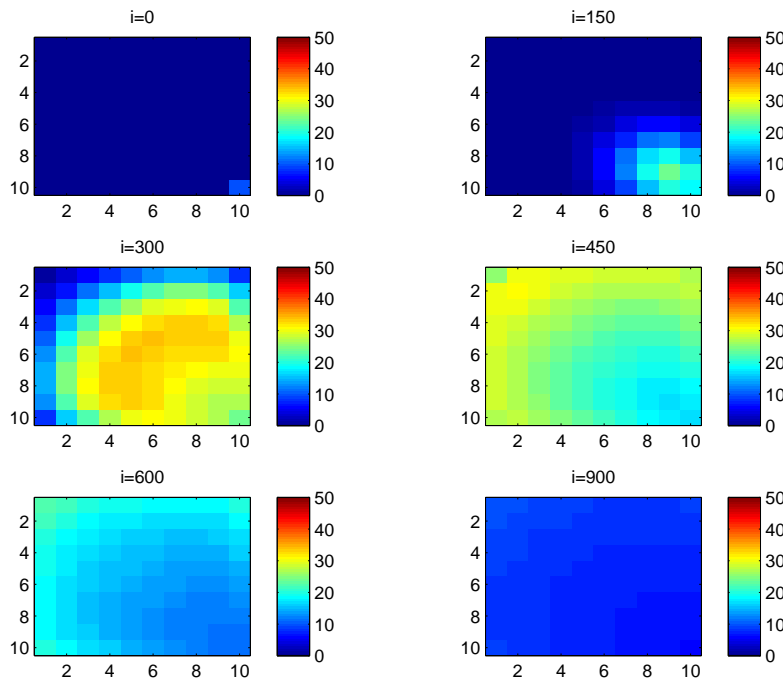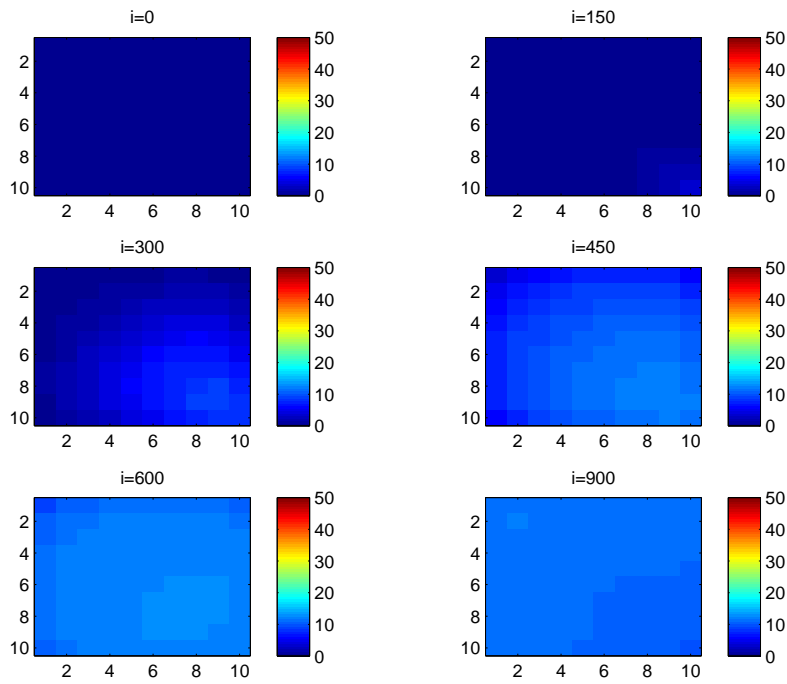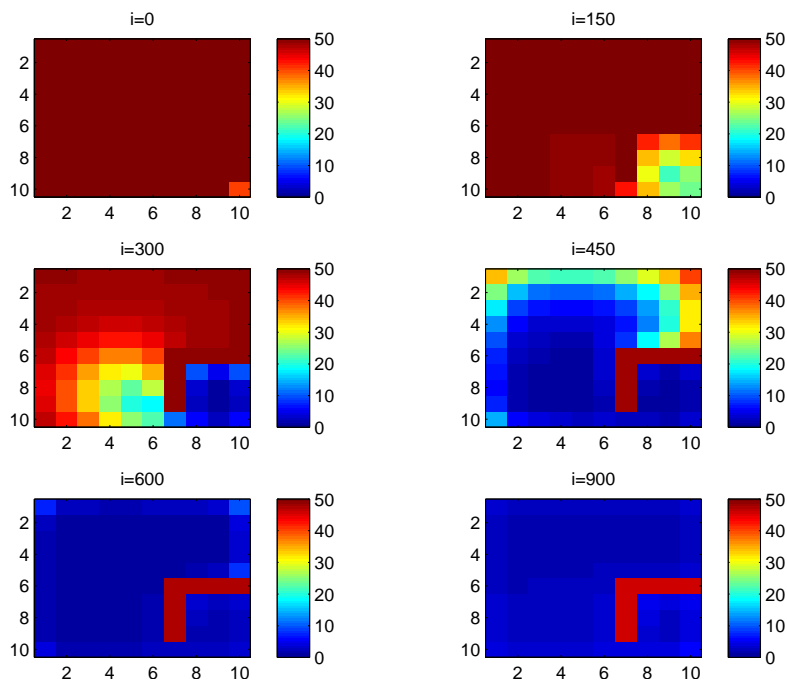

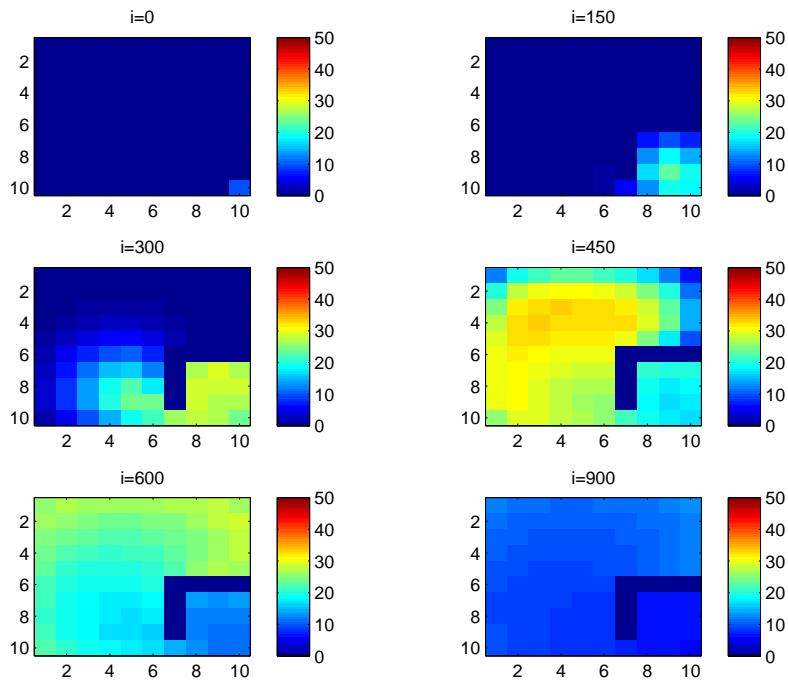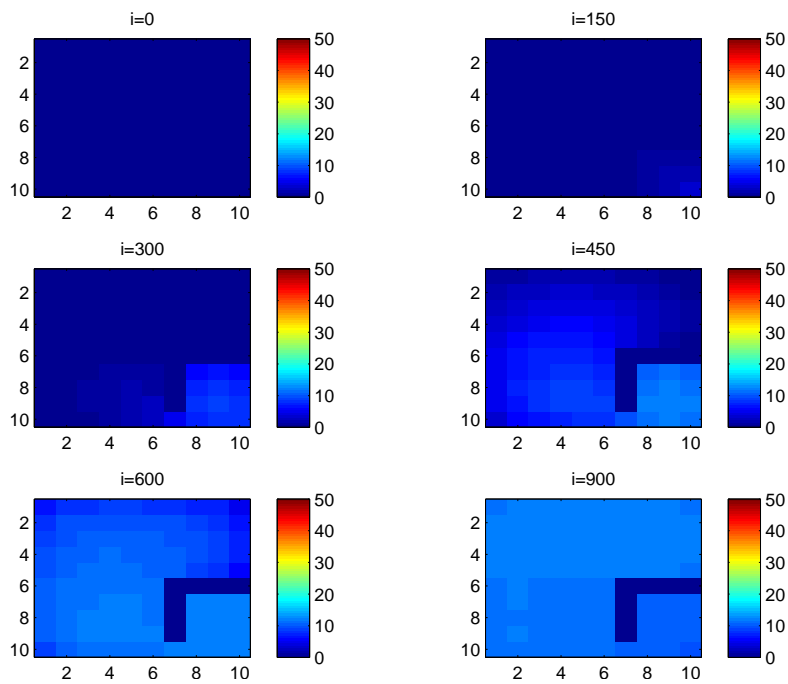
Fig. 2. $I^{C_{pq}}$ **behavior in the absence of controls**

Fig. 3. $R^{C_{pq}}$ **behavior in the absence of controls.**

Fig. 4. $S^{C_{pq}}$ **behavior in the presence of optimal controls**

Fig. 5. $I^{C_{pq}}$ **behavior in the presence of optimal controls**

Fig. 6. $R^{C_{pq}}$ **behavior in the presence of optimal controls**

In Fig. 5, the number $I^{C_{pq}}$ has not changed in the controlled patch at $i = 150$ and remained zero even in cells at the borders of the patch. At $i = 300$, $I^{C_{pq}}$ remains zero in all cells of the patch while this number has not changed significantly and it has not even exceeded 25 infected individuals at the left-side border and it remains under 10 at distant cells. This shows the importance of the travel-blocking vicinity optimal control strategy in protecting even distant cells to the controlled chain as we see in Fig. 2 that $I^{C_{pq}}$ increased to higher numbers in same cells. Similar conclusions to this last one, can be deduced at $i = 450$. As for further instants, $I^{C_{pq}}$ in the patch has increased only by three individuals.

In Fig. 6, $R^{C_{pq}}$ in the patch remains zero and similar behavior of $R^{C_{pq}}$ to Fig. 3 is shown in most times except for some cells at/near the borders of the controlled patch and in vicinities of these borders, and which proves again that the travel-blocking vicinity optimal control strategy protects the patch, its borders and even delay the impact of the epidemic at distant cells.

5 CONCLUSION

In this paper, we proposed a multi-regions SIRS discrete epidemic model to describe the spatial-temporal spread of an epidemic, and we tried to investigate the effectiveness of the travel-blocking vicinity optimal control strategy on a group of regions or patch P that belongs to a global domain of interest Ω. Based on the numerical results exhibited in cellular simulations, we demonstrated that movements restrictions of infected populations coming from the vicinity of P, have not only kept this patch safe, but have even protected its borders for some time, and the infection has been delayed in very distant cells.

ACKNOWLEDGEMENTS

COMPETING INTERESTS

Authors have declared that no competing interests exist.

References

[1] Chaturvedi O, Masupe S, Masupe T. SIRS model for the dynamics of non-typhoidal salmonella epidemics. International Journal of Computational Engineering Research. 2013;03(10).

[2] Mukhopadhyay BB, Tapaswi PK. An SIRS epidemic model of Japanese encephalitis. International Journal of Mathematics and Mathematical Sciences. 1994;17(2):347-355.

[3] Zhao H, Jiang J, Xu R,Ye Y. SIRS model of passengers panic propagation under self-organization circumstance in the subway emergency. Mathematical Problems in Engineering; 2014.

[4] Li T, Li Y, Hethcote HW. Periodic traveling waves in SIRS endemic models. Mathematical and Computer Modelling. 2009;49(1-2):393-401.

[5] El-Saka HAA. The fractional-order SIR and SIRS epidemic models with variable population size. Mathematical Sciences Letters. 2013;2(3):195.

[6] Sekiguchi M. Permanence of a discrete SIRS epidemic model with time delays. Applied Mathematics Letters. 2010;23(10):1280-1285.

[7] Sekiguchi M, Ishiwata E. Global dynamics of a discretized SIRS epidemic model with time delay. Journal of Mathematical Analysis and Applications. 2010;371(1):195-202.

[8] El Kihal F, Abouelkheir I, Rachik M, Elmouki I. Optimal control and computational method for the resolution of isoperimetric problem in a discrete-time SIRS System. Mathematical and Computational Applications. 2018;23(4):52.

[9] Zakary O, Rachik M, Elmouki I. On the analysis of a multi-regions discrete SIR

epidemic model: An optimal control approach. International Journal of Dynamics and Control. 2016;1-14.

[10] Zakary O, Rachik M, Elmouki I. A new analysis of infection dynamics: multi-regions discrete epidemic model with an extended optimal control approach. International Journal of Dynamics and Control. 2016;1-10.

[11] Zakary O, Rachik M, Elmouki I. A new epidemic modeling approach: Multi-regions discrete-time model with travel-blocking vicinity optimal control strategy. Infectious Disease Modelling. 2017;2(3):304-322.

[12] El Kihal F, Rachik M, Zakary O, Elmouki I. A multi-regions SEIRS discrete epidemic model with a travel-blocking vicinity optimal control approach on cells. Int. J. Adv. Appl. Math. Mech. 2017;4(3):60-71.

[13] Abouelkheir I, Rachik M, Zakary O, Elmouki I. A multi-regions SIS discrete influenza pandemic model with a travel-blocking vicinity optimal control approach on cells. American Journal of Computational and Applied Mathematics. 2017;7(2):37-45.

[14] Chouayakh K, Rachik M, Zakary O, Elmouki I. A multi-regions SEIS discrete epidemic model with a travel-blocking vicinity optimal control approach on cells. Journal of Mathematical and Computational Science. 2017;7(3):468-484.

[15] Zakary O, Rachik M, Elmouki I. A multi-regional epidemic model for controlling the spread of Ebola: awareness, treatment, and travel-blocking optimal control approaches. Mathematical Methods in the Applied Sciences; 2016.

[16] Zakary O, Larrache A, Rachik M, Elmouki I. Effect of awareness programs and travel-blocking operations in the control of HIV/AIDS outbreaks: A multi-domains SIR model. Advances in Difference Equations. 2016;1:1-17.

[17] Abouelkheir I, El Kihal F, Rachik M, Zakary O, Elmouki I. A multi-regions SIRS discrete epidemic model with a travel-blocking vicinity optimal control approach on cells. Br. J. Math. Comput. Sci. 2017;20(4):1-16.

[18] Zakary O, Rachik M, Elmouki I, Lazaiz S. A multi-regions discrete-time epidemic model with a travel-blocking vicinity optimal control approach on patches. Advances in Difference Equations. 2017;1:120.

[19] Sethi SP, Thompson GL. What is optimal control theory? Springer, US. 2000;1-22.